A parametric study of CO_2 capture from gas-fired power plants using monoethanolamine (MEA)

Salman Masoudi Soltani[a,b], Paul S. Fennell[a] and Niall Mac Dowell[c,d,]*

[a]Department of Chemical Engineering, Imperial College London, South Kensington Campus, London SW7 2AZ, United Kingdom
[b]Department of Mechanical, Aerospace and Civil Engineering, Brunel University London, Uxbridge UB8 3PH, United Kingdom
[c]Centre for Environmental Policy, Imperial College London, South Kensington Campus, London SW7 1NA, United Kingdom
[d]Centre for Process Systems Engineering, Imperial College London, South Kensington Campus, London SW7 2AZ, United Kingdom

*Corresponding author's Tel: +44 (0)20 7594 9298

Abstract

The value of dispatchable, low carbon thermal power plants as a complement to intermittent renewable energy sources is becoming increasingly recognised. In this study, we evaluate the performance of post-combustion CO_2 capture using monoethanolamine (MEA) retrofitted to a 600 MW CCGT, with and without exhaust gas recycle (EGR). Our results suggest that the EGR ratio plays a primary role in the regeneration energy penalty of the process. We contrast a gas-CCS process with its coal counterpart and show that whilst CCGTs have a greater energy penalty per tonne of CO_2 captured than coal (*i.e.*, $GJ/t_{CO_2}^{Gas} > GJ/t_{CO_2}^{Coal}$), owing to the high thermal efficiencies of CCGTs relative to coal-fired power plants, the energy penalty per MWh of low carbon energy generated is lower for gas than it is for coal (*i.e.*, $GJ/MWh^{Gas} < GJ/MWh^{Coal}$), making CCGT-CCS an attractive choice for low carbon electricity generation.

Keywords

CO_2 Capture, post-combustion capture, Aspen Plus, CCGT, Gas CCS, gas-fired power plant

1 Introduction

A significant reduction in total CO_2 emissions is essential to limit the average global temperature rise to 2 °C by the end of this century (Luo, et al., 2015). In December 2015, the so-called "COP21" agreement has identified the highly ambitious aspiration of limiting temperature rise to 1.5 °C (United Nations, 2015). Fossil fuels including coal and gas are currently primary sources of CO_2 emissions to the atmosphere and thus, a key contributor to anthropogenic climate change. Power generation using fossil fuels dominates the world's energy landscape and currently contributes approximately 25% of total global greenhouse gas emissions (US Environmental Protection Agency, 2016), and despite a rapid expansion of the role of renewable power, fossil energy is likely to play a dominant role in the world's energy landscape for some time to come.

In this context, the role of natural gas as part of a transition to a low carbon energy system is becoming increasingly important[1], as presented in Table 1, compared to coal-fired power generation, natural gas-fired power plants emit 50 to 60% less CO_2 on a per MWh basis (National Energy Technology Laboratory (NETL), 2013).

Table 1: The average kg of CO_2 emitted per MWh of energy for various fuels from 2007 to 2014 (U.S. Energy Information Administration, 2015)

Fuel Type	kg_{CO2}/MWh_{th}	kg_{CO2}/MWh_{e}
Coal (bituminous)	318.34	938.93
Coal (lignite)	333.36	984.29
Coal (subbituminous)	331.66	979.76
Natural gas	250.72	553.38

However, combined cycle gas turbines (CCGT) are not themselves low carbon – they're just lower carbon than coal, and in a low carbon world, they will also need to be decarbonised via CCS (Heuberger, et al., 2016). In the context of decarbonising CCGTs, post-combustion capture processes are generally considered the most appropriate for this purpose (Boot-Handford, et al., 2014), although chemical looping combustion technologies are also especially promising (Hassan, et al., 2017). Other recent studies also consider the oxy-combustion of natural gas in CCGTs (Climent Barba, et al., 2016).

Abu-Zahra et al. (2007b) performed a detailed evaluation of amine-based post-combustion CO_2 capture applied to a 600 MW bituminous coal fired power plant using monoethanolamine (MEA) as the working solvent. They achieved a reduction in energy consumption from 3.9 to 3.0 GJ/t_{CO2} by using a higher concentrations of MEA (*i.e.* 40 wt%). Although this is a significant

---

[1] Such as in the UK, where, at the time of writing, there is the ambition to close all unabated coal-fired power stations and replace this capacity with gas-fired capacity (Department of Energy & Climate Change, 2015).

improvement, it is still limited in industrial applications due to corrosion and solvent degradation issues. Sharifzadeh and Shah (2015) presented a comparative study of MEA and an amine-promoted buffer salt (APBS) in CO_2 capture from gas-fired power plants. They studied three different scenarios and compared their results with available pilot plant data. In their work, they utilized an MEA solution (30 wt%) to model the capture process unit. They validated their work by comparing their results with a pilot-plant data and a flue gas CO_2 concentration of 6.7 wt% in their various runs. Therefore, lower concentrations of CO_2 in the flue gas were not considered in their study. Llano-Restrepo and Araujo-Lopez (2015) presented a comprehensive and recent list of research works reported in the literature on the absorber models used for the simulation of carbon dioxide capture in MEA solution for fossil fuel-fired power plants. The energy penalty for a conventional capture unit integrated with a coal-fired power plant is approximately between 3.2 to 4.2 ${GJ}/{t_{CO_2}}$. For a CO_2 capture unit being fed by the flue gas generated in a gas-fired power plant, Ogawa (2013) reported a reboiler-based energy penalty in order of 3.3 ${GJ}/{t_{CO_2}}$corresponding to a carbon recovery of only 76.5%. However, these researchers did not present any power plant de-rating figures with a retrofitted CCS unit.

One of the main challenges of using amine-based post combustion capture technologies is amine degradation due to the presence of oxygen in the flue gas (Mertens, et al., 2013). This is especially of concern for the exhaust gas of a CCGT which contain up to 10-12 mol% oxygen, relative to coal-fired power plants where an O_2 concentration of 5 – 6 mol% would be the norm. Given that amine degradation costs increase the variable operating and maintenance costs, this could potentially result in an unviable capture process. In order to minimise oxygen concentration and maximise CO_2 concentration in the exhaust gas from a CCGT power plant, a portion of the exhaust gas exiting the heat recovery steam generator (HRSG) is recycled back into the inlet of the gas compressor of the turbine. This technique is known as Exhaust Gas Recycle (EGR) and has its origin in the operation of gas compression equipment (Loud & Slaterpryce, 1991). The increase in CO_2 concentration leads to a lower energy of regeneration and thus, lower capital and electricity cost as well as CO_2 avoidance costs in the short, medium and long run (Li, et al., 2011) (Adams & Mac Dowell, 2016). Importantly, it has been reported that the application of EGR to a CCGT causes little variation in the performance of the turbine

(Canepa, et al., 2013). This implies that the EGR strategy is potentially applicable to CCS retrofit scenarios. However, it is worth noting that due to the change in the thermodynamic properties of the gas as a result of the change in CO_2 concentration, the output power from the gas turbine can be adversely affected. This owes to the lower heat capacity of CO_2 compared to air which consequently, lowers the outlet temperature of the combustor (Akram, et al., 2013). These issues must be addressed for large-scale applications. In a recent study, Ali et al. (2016), carried out a techno-economic analysis of a CCGT with various EGR percentages (*i.e.* 20%, 35% and 50%) in a pilot-scale capture unit (30 wt% MEA, a lean loading of 0.2 and a 90% capture rate). They investigated the effect of various EGR ratios on the liquid-to-gas ratios and the subsequent effect on the CO_2 concentration in the inlet flue gas to the absorber. Akram et al. (2016) also investigated the effect of EGR ratio on the performance of a pilot-scale capture unit. They considered flue gas CO_2 concentrations in the range of 5.5 to 9.9 vol%. These researchers observed an increase in CO_2 concentration in the flue gas with an increase in the EGR ratio leading to a reduction in the specific reboiler duty by 7.1% per unit percentage increase in CO_2 concentration.

Post-combustion CO_2 capture will impose a well-known energy penalty upon the power plant with which it is integrated (Hanak, et al., 2015). This leads to a net efficiency reduction on the power plant on the order of 10–12%-pts, primarily due to the energy required for solvent regeneration, followed by CO_2 compression and other auxiliary energy consumption, *i.e.*, solvent and cooling water pumps together with the blower (Linnenberg, et al., 2012). Solvent regeneration accounts for approximately 60% of the energy penalty associated with the operation of a post-combustion CO_2 capture process (Kothandaraman, et al., 2009). For MEA-based CO_2 capture applied to a CCGT, depending on the capture rate, solvent flow rate and reboiler duty, the energy of regeneration is typically on the order of 4 to 5 GJ/tCO_2, *i.e.*, somewhat greater than might be expected for an equivalent coal-fired power station (Kehlhofer, et al., 2009). The utilisation of advanced amines, such as piperazine, has the potential to reduce this cost (Kvamsdal, et al., 2014) with recent pilot plant data reporting an energy cost in the range 2.1-2.9 GJ/tCO_2 (Lin, et al., 2016).

There have been several efforts to describe the chemical absorption of post combustion CO_2 from the flue gases of both coal- and gas-fired power plants. These models have either been developed on the assumption of equilibrium or rate-based mass transfer with some having been validated on pilot-scale plants (Mac Dowell, et al., 2013; Dutta, et al., 2017; (Sherman, et al., 2016; Norouzbahari, et al., 2016; Oko, et al., 2015). Although rate-based process simulation is well-known to provide more insight into the absorption process enabling the engineers to size the equipment and evaluate the process operating conditions more accurately (Sharifzadeh & Shah, 2015; Mac Dowell, et al., 2013; Krishnamurthy & Taylor, 1985b; Krishnamurthy & Taylor, 1985a), equilibrium simulation, owing to its relative simplicity, provides useful insight on the viability of the process if used astutely. Therefore, we have adopted an equilibrium-based modelling approach in order to simulate our process.

Among various modelling approaches, the parametric method has been adopted by many researchers. For example, Qi (2007) carried out a parametric study in order to simulate an MEA-based CO_2 absorption plant for a CCGT (3.73 mol% CO_2 in the inlet flue gas). He considered total CO_2 capture and the reboiler energy consumption as the key performance indicators (KPIs). He reported that the efficiency of the CCGT would drop by 8 pt-% from 58% to 50% by retrofitting a post-combustion capture unit. It was shown that an 85% capture rate was associated with an energy consumption of 3.7 GJ/tCO_2.

In this study, we evaluate the performance of a post combustion CO_2 capture plant applied to the exhaust gas of a 600 MW CCGT power plant using a range of EGR ratios with concurrent consideration of other operational parameters. The remainder of this paper is set out as follows; we first describe our modelling approach in detail, and then present the results of our parametric analysis. We conclude with some discussion and a comparison of coal- and gas-CCS processes.

2 Model Development

Throughout this work, we have employed the electrolyte NRTL (electrolyte non-random-two liquid) (Chen & Evans, 1986) to model the liquid phase and the SRK equation of state (EoS) (Soave, 1972) to describe the vapour phase.

The following section briefly outlines the methods used in order to integrate the absorption, aqueous-phase reactions and thermodynamic mechanisms involved in the MEA-CO_2-H_2O systems into the model. In the following sections we concisely review the fundamentals behind the thermodynamic framework employed in this study.

2.1 Absorption and Reaction Mechanisms (chemical equilibria)

The absorption process begins with the dissolution of gaseous carbon dioxide molecules into the liquid.

$$CO_2(g) \longrightarrow CO_2(aq) \text{ (1)}$$

In the aqueous solution of MEA-H2O-CO$_2$, the dissolved CO$_2$ will then undergo a series of reactions resulting in the formation of a number of ionic species. The governing reactions in the in this electrolyte system are presented below:

$$2H_2O \overset{K_2}{\leftrightarrow} H_3O^+ + OH^- \text{ (2)}$$

$$CO_2 + 2H_2O \overset{K_3}{\leftrightarrow} H_3O^+ + HCO_3{}^- \text{ (3)}$$

$$HCO_3{}^- + H_2O \overset{K_4}{\leftrightarrow} H_3O^+ + CO_3{}^{2-} \text{ (4)}$$

$$MEAH^+ + H_2O \overset{K_5}{\leftrightarrow} MEA + \ H_3O^+ \text{ (5)}$$

$$MEACOO^- + H_2O \overset{K_6}{\leftrightarrow} MEA + HCO_3{}^- \text{ (6)}$$

In the reactions listed above, reaction (2) describes water hydrolysis, reaction (3) shows the formation of bicarbonate in water and reaction (4) illustrates the dissociation of bicarbonate into carbonate ions in the presence of liquid water. Reactions (5) and (6) describe how molecular MEA reacts with CO$_2$ in aqueous solution.

The equilibrium constants for reactions 1-5 are defined as:

$$K(T) = \prod \alpha_i{}^{\nu_i} = \prod (m_i . \gamma_i)^{\nu_i} \text{ : molar basis (7)}$$

or

$$K(T) = \prod (x_i . \gamma_i)^{\nu_i} \text{ : mole fraction basis (8)}$$

In equations (7) and (8), $K(T)$ is the temperature-dependent equilibrium constant; α_i is the activity of species$i$; ν_i is the stoichiometric constant of species i; m_i is the molality of species i and γ_i is the activity coefficient of species i and x_i is the mole fraction of species i. Whilst an equilibrium description of these reactions is unlikely to be adequate for detailed process design, this approach is deemed appropriate for a parametric study of the kind presented here.

The original electrolyte NRTL model, a $\gamma - \varphi$ model, was initially developed for a single solvent and a completely-dissociated electrolyte (Renon & Prausnitz, 1968) and was subsequently generalized so as to be applicable to multi-component aqueous systems (Chen & Evans, 1986).

Since the activity coefficient, γ_i, for any species (ionic or molecular, solute or solvent) is calculated from the partial derivative of the excess Gibbs free energy with respect to mole number, n_i therefore (Dash, et al., 2011) :

$$ln\gamma_i = \frac{1}{RT}\left[\frac{\partial(n_t G^{*ex})}{\partial n_i}\right]_{T,P,n_{j\neq i}} \quad (9)$$

Where $i, j = molecule, cation, anion\ species$

Finally, equation (9) leads to:

$$ln\gamma_i{}^{*} = ln\gamma_i{}^{*PDH} + ln\gamma_i{}^{*NRTL} + ln\gamma_i{}^{*BORN} \quad (10)$$

In the eNRTL property method, the temperature-dependent reaction equilibrium constants (K_i) are calculated using the Aspen Plus built-in equation:

$$ln(K_i) = a_i + \frac{b_i}{T} + c_i\, ln(T) + d_i T \quad (11)$$

2.2 Vapour-Liquid Thermodynamic System (phase equilibria)

An extended Henry‘s law is employed to represent the behaviour of solutes such as CO_2 (Mondal, et al., 2015):

$$y_i.\varphi_i.P = x_i.\gamma_i.H_i{}^{P^0}.\exp[\frac{V_i{}^{\infty}(P-P_s{}^0)}{RT}] \quad (12)$$

Similarly, for the solvents, an extended Raoult’s law is used (Mondal, et al., 2015):

$$y_s.\varphi_s.P = x_s.\gamma_s.P_s{}^0.\varphi_s{}^0.\exp[\frac{V_s(P-P_s{}^0)}{RT}] \quad (13)$$

In equations (12) and (13), the exponential terms are the Poynting factors or corrections for moderate pressure and are derived from integration forms by assuming $V_i{}^{\infty}$ and V_s to be constant over the pressure range. Also, y_i and y_s are the mole fractions of species i and s in the gas phase; φ_i and φ_s are vapour phase fugacity coefficients for species i and s; P is the total pressure; x_i and x_s are the mole fractions of species and in the liquid phase; γ_i and γ_s are the liquid phase activity coefficients for species i and s; $H_i^{P^0}$ and $P_s{}^0$ are respectively the Henry's constant of i in the amine solution and saturation pressure of component s; $\varphi_s{}^0$ is the fugacity coefficient of s under saturation condition; V_i^∞ and V_s are the partial molar volume of solute at infinite dilution and the molar volume of the solvent s; $P_s{}^0$ is the vapour pressure of solvent at saturated conditions.

2.3 Post Combustion CO_2 Capture Process Flowsheet

Many chemical processes such as natural gas sweetening, synthesis gas purification, manufacturing of nitric acid, chlorination, hydrogenation and carbon capture employ a gas scrubbing process to treat the generated flue gas or improve the products' quality (Gaspar & Fosbøl, 2015). The absorption and desorption processes usually take place in gas–liquid contactors. Figure 1 presents the flowsheet that was developed in this work.

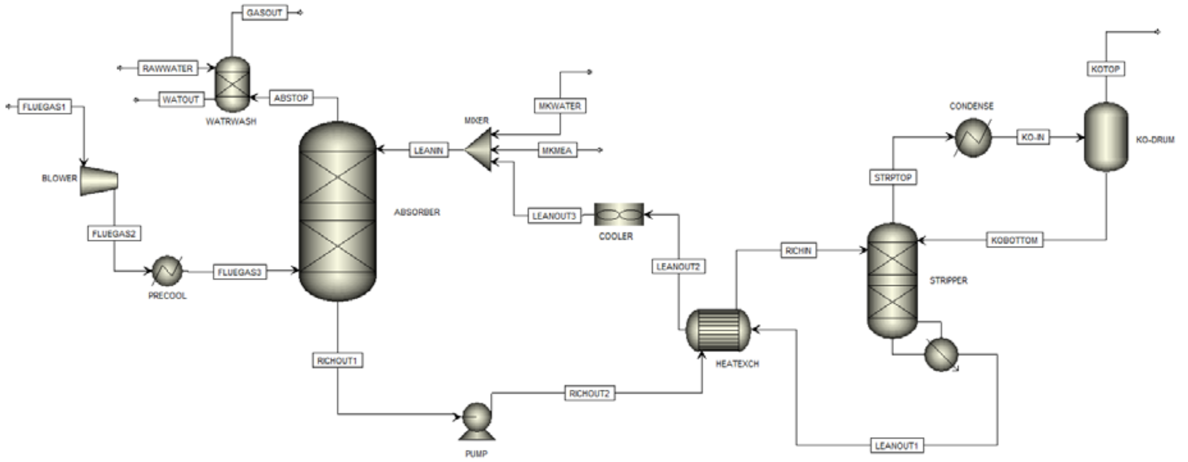

Figure 1: Schematic of the amine-based carbon capture process flow diagram

The operating conditions of different units in the flowsheet are reviewed in Table 2.

Table 2: The operating conditions of the main units in the simulated flowsheet

Design Specification	Specified Value
Absorber operating pressure (bar_a)	1.1 (isobaric)
Absorber's no. of ideal stages	15
Stripper's operating pressure (bar_a)	2 (isobaric)
Stripper's no. of ideal stages	10
Condenser's outlet temperature (°C)	30
Knock-out drum pressure (bar_a)	2
Knock-out drum temperature (°C)	30

Water-wash column pressure (bar_a)	1.1
Blower ΔP (bar_a)	0.1
Precooler's outlet temperature (°C)	40
Assumption for pressure drop in pipes and equipment (bar_a)	0

In addition to the above, the key process specifications for the inlet streams are presented in Table 3.

Table 3: The main stream values in the base-case flowsheet

Parameter	**Inlet Flue Gas**	**Inlet Lean Solvent**
CO_2 content (mol %)	4, 6, 8	N/A
CO_2 Loading Range	N/A	0.15 - 0.35
Lean Solvent Concentration (wt %)	N/A	15, 20, 25, 30
Temperature (°C)	120	40
Pressure (bar_a)	1.05	1.1

The concentration of CO_2 (and other species) in the flue gas are modelled to represent various EGR ratios (Adams & Mac Dowell, 2016) in a gas-fired power plant. The compositional analysis of the inlet flue gas used in this simulation is given in Table 4.

Table 4: Inlet flue gas compositions studied in this work (Adams & Mac Dowell, 2016)

Inlet Flue Gas Composition (mol%)	**EGR Ratio% = 0**	**EGR Ratio% = 20**	**EGR Ratio% = 40**
CO_2	4	6	8
O_2	12	9	5
H_2O	7	7	7
N_2	77	78	80

3 Results and Discussions

3.1 Effect of Lean Loading on CO_2 Capture Energy Efficiency

The effect of lean loading on reboiler-based energy consumption for various EGR ratios and amine concentrations is illustrated in Figure 2. It is evident that for all combinations of MEA concentration and exhaust gas CO_2 concentration there is a pronounced minimum in the energy of regeneration.

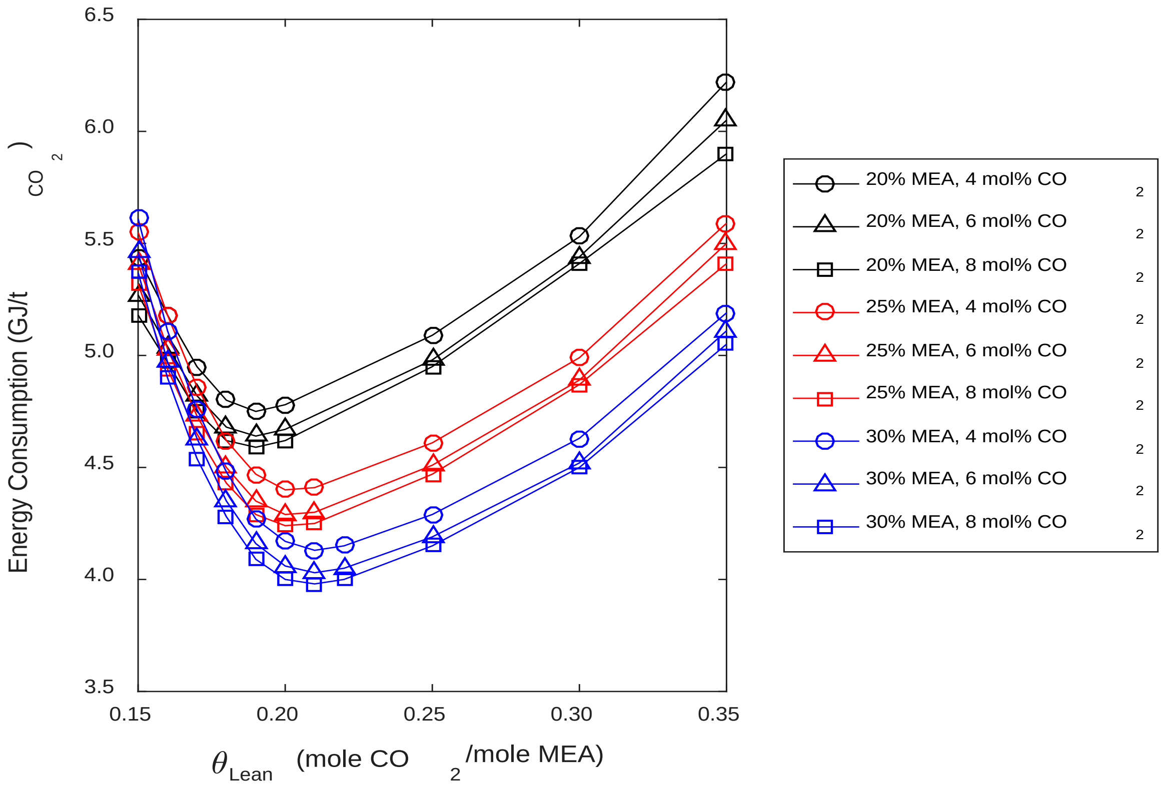

Figure 2: Effect of lean loading on energy consumption (90% CO_2 capture, rich loading: 0.5)

Holding the degree of CO_2 capture constant at 90% and initiating the parametric sweep with a θ_{Lean} of 0.35, reducing θ_{Lean} initially reduces into a reduction in lean solvent flow rate and a commensurate reduction in the energy cost of regeneration, consistent with the observations reported by Alhajaj et al. (2016). It can be observed that, for the range of MEA concentrations and EGR evaluated here, y_{CO2} plays a secondary role in determining energy of regeneration – the amine concentration exerts a more significant effect, with a reduction in amine concentration shifting the location of the energy minimum towards lower values of θ_{Lean}. As a secondary effect, an increase in the EGR ratio consistently reduces the energy consumption. Therefore, it would appear sensible to maximise both amine concentration and EGR ratios. However, 30 wt% MEA is commonly considered an upper limit owing to concerns of equipment corrosion (Abu-Zahra, et al., 2007a) and the utility of EGR as a strategy is also limited to approximately 35-40% (Merkel, et al., 2013) owing to the fact that at elevated EGR ratios greater than 40%, the O_2 concentration in the combustion chamber drops below 16% resulting in inefficient fuel conversion (Li, et al., 2011).

The energy for solvent regeneration can be decomposed to three primary contributing factors (Oexmann & Kather, 2010):

1. The energy required for the vaporisation of water and thus, the generation of steam (*i.e.* latent heat) – which is dependent on CO_2 and water partial pressures in equilibrium with the liquid phase
2. The sensible heat of the solvent which is required to be supplied in order to increase the liquid temperature to that of the reboiler. This is linked to the solvent flow rate.
3. The heat of desorption of CO_2 from the rich solvent. This primarily depends on the type of solvent used. Also, it is directly affected by the CO_2 loading of the desired lean solvent.

Thus, the total reboiler heat duty is not simply a function of CO_2 desorption energy but comprises two other very important terms, namely the sensible heat and heat of water evaporation. Therefore the total required regeneration energy in the stripper can be shown as (Mac Dowell & Shah, 2013; Young, et al., 2012; Oexmann & Kather, 2010):

$$q_{reg} = \frac{H_{reboiler}}{\dot{m}_{CO_2}} = q_{sen} + q_{vap,H_2O} + q_{abs,CO_2} \quad (14)$$

Where q_{reg} is the sensible energy, q_{vap,H_2O} is water evaporation energy, q_{abs,CO_2} is the CO_2 absorption energy, $H_{reboiler}$ is the heat duty of the reboiler and $\dot{m}_{CO_2}$ is the mass flow rate of CO_2. The CO_2 heat of absorption comprises three parts (Oexmann & Kather, 2010): non-ideal mixing; dissolution of gas into the liquid and chemical reaction.

In order to provide some insight into the physical factors which drive the shape of the curves presented in Figure 2, the contribution of each energy term to the stripper's total heat duty is presented in Figure 3 .

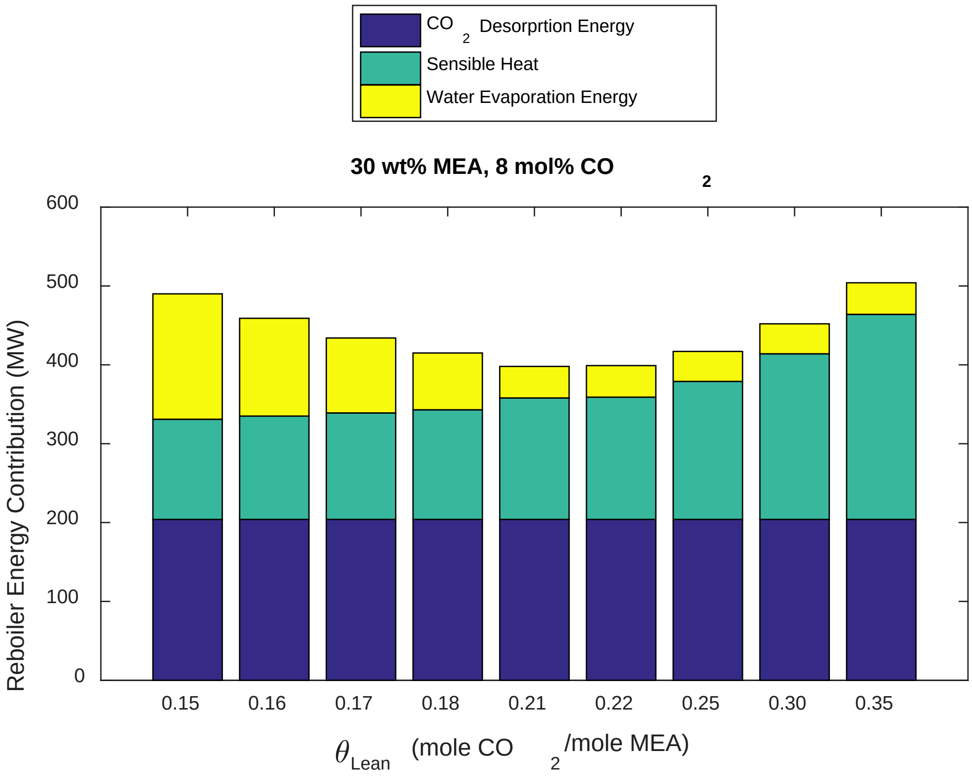

Figure 3: Reboiler energy breakdown for various amine concentrations and EGR ratios

As can be observed, the amount of energy required to actually recover the CO_2 remains approximately constant – which makes intuitive sense. At higher values of lean loading, more energy is required for sensible heating owing to increased quantity of solvent required to maintain a constant degree of capture. However, at lower values of lean loading, the vapour liquid equilibrium conditions shift, and an increased amount of energy is spent producing water vapour, consistent with previous observations in the literature (Oexmann & Kather, 2010). These trends were also observed by Abu-Zahra et al. (2007b) for a corresponding coal-fired power plant.

The variation of solvent flow rate for various lean loadings is shown in Figure 4.

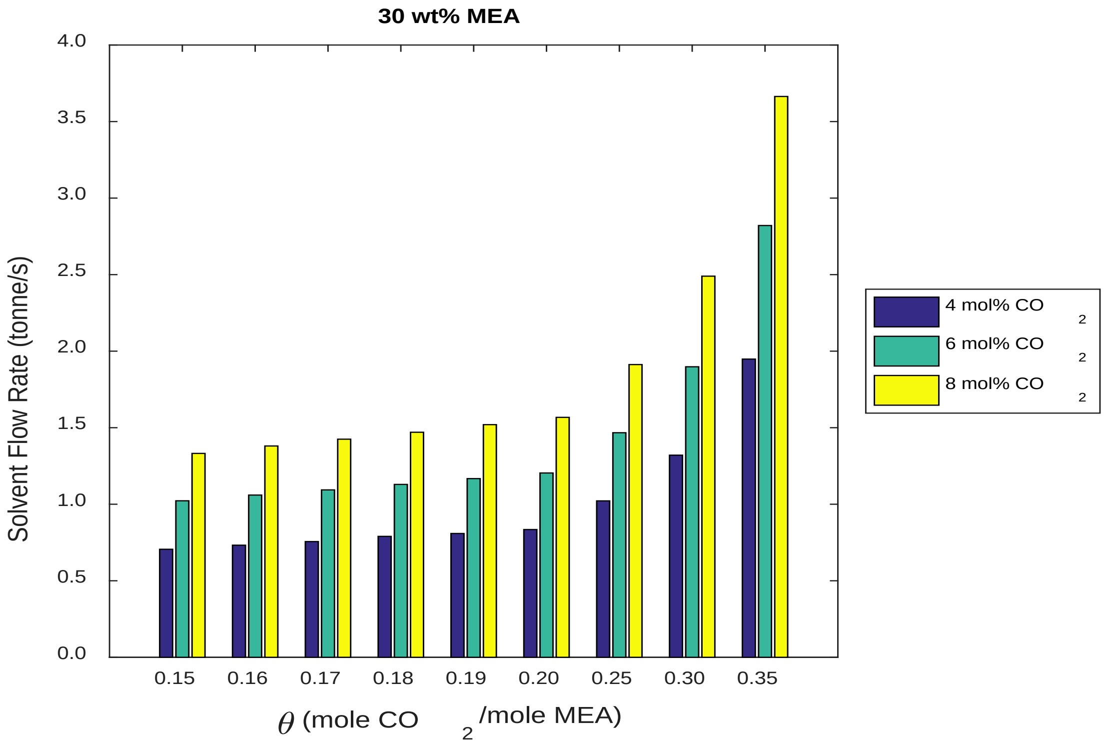

Figure 4: Effect of lean loading on lean solvent flow rate (90% CO_2 capture)

It can be observed that with an increase in loan loading, an increased solvent is required to achieve the constant CO_2 capture of 90%, as there is a reduced carrying capacity in the working solvent. This is similar to what has been observed in previous work (Alhajaj, et al., 2016; Adams & Mac Dowell, 2016).

3.2 Effect of MEA Concentration on CO_2 Capture Energy

In Figure 5, the effect of MEA concentration in the lean solvent on the reboiler-based energy efficiency of the process has been illustrated for various lean loadings and EGR ratios.

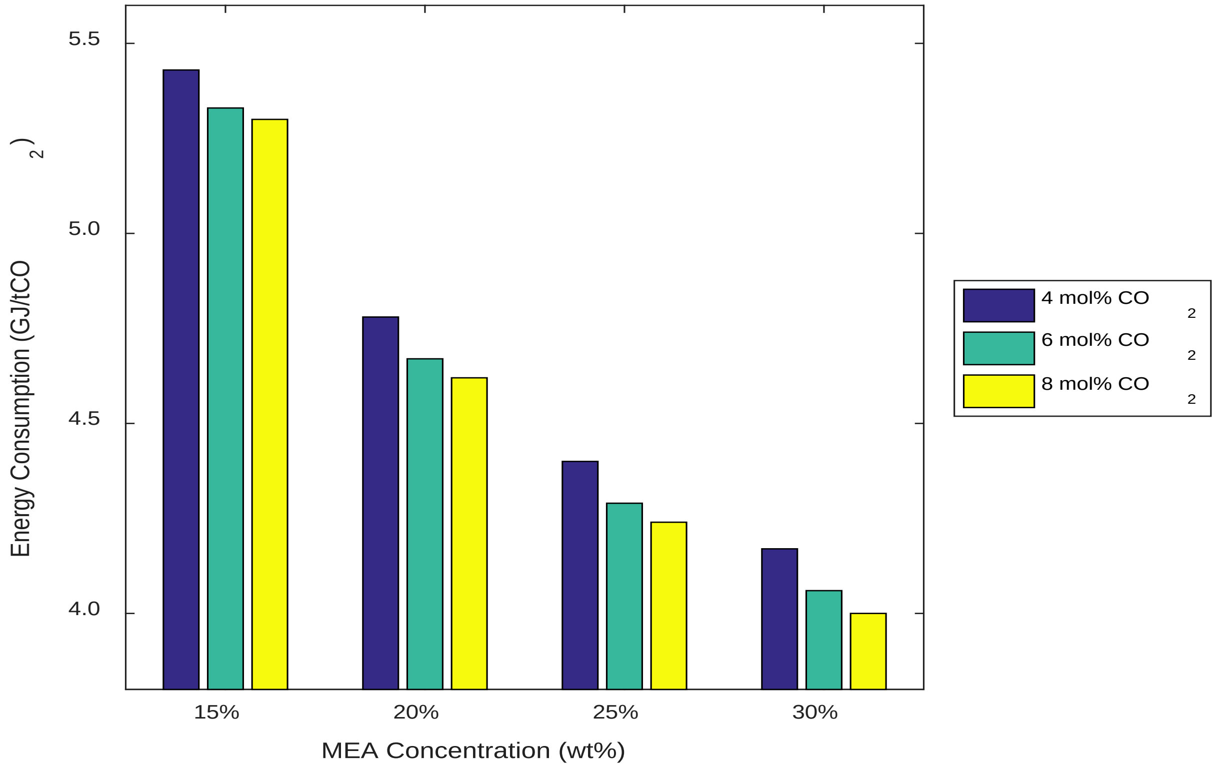

Figure 5: Effect of MEA concentration in lean solvent on the reboiler energy efficiency (90% CO_2 capture, rich loading: 0.5, 0.20 lean loading)

Figure 5 shows that with an increase in MEA concentration, leading to a reduction in solvent flow rates, the reboiler energy consumption is reduced. This trend is consistent across all values of y_{CO2}. It may also be observed from Figure 5 that at a constant MEA concentration, an increase in gas phase CO_2 concentration leads to a second order reduction in energy consumption. The minimum is achieved with an MEA concentration of 30 wt%, a lean loading of 0.20 and an EGR of 40% (*i.e.* 8 mol% CO_2 in the flue gas) - here the energy of regeneration is 3.98 GJ/tCO_2.

3.3 Effect of CO_2 Capture Rate on Reboiler Duty

The basic operating conditions of the process (Table 3) were kept constant during the simulation. In order to be able to perform a parametric study on the effect of reboiler heating duty on CO_2 capture, the inlet flue gas composition, lean loading and the MEA concentration in lean loading were kept constant. However, the capture was manipulated by a varying lean solvent flow rate. The effect of the reboiler duty and its corresponding steam consumption on the total carbon dioxide capture percentage from the flue gas is illustrated in Figure 6.

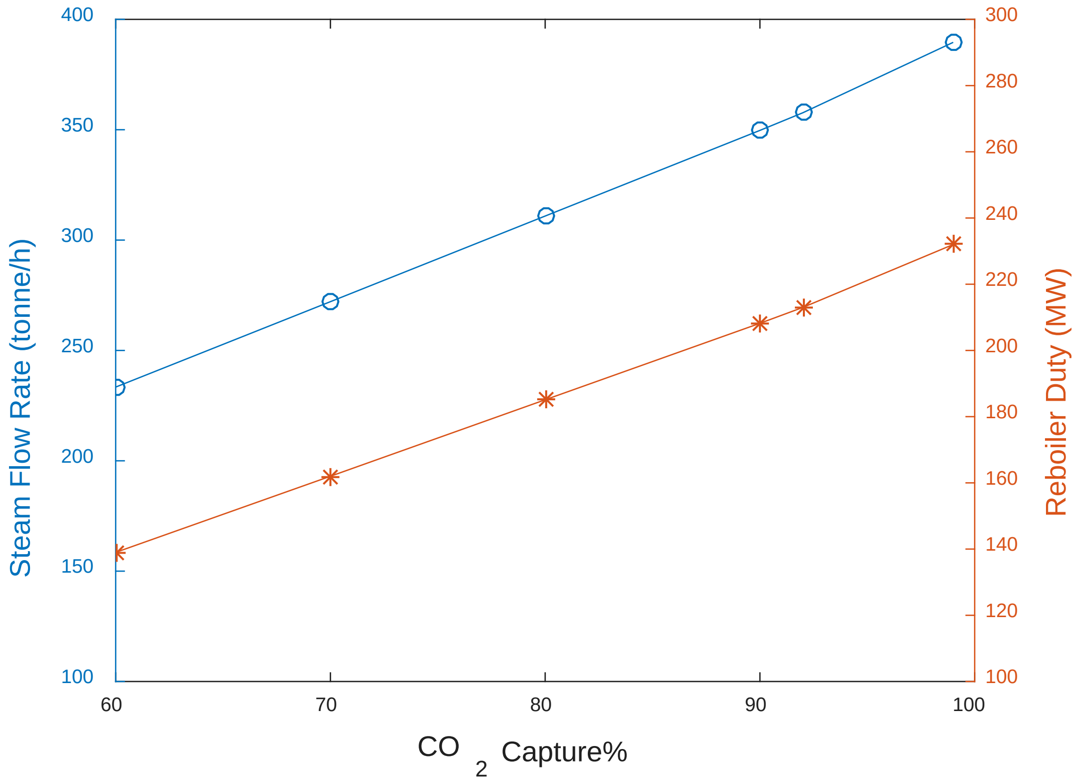

Figure 6: Effect of reboiler duty on the recovery of CO_2 from the flue gas (Inlet flue gas with 4 mol% CO_2; Lean Loading: 0.21; 30 wt% MEA; utility steam: saturated steam at 140 °C bled from the IP-LP turbines crossover.)

Figure 6 shows a linear increase in the reboiler duty with increasing CO_2 capture.

As discussed previously, the energy of regeneration includes that required for vaporisation of water, CO_2 desorption and that required to raise the inlet solvent temperature to that of the reboiler (Oexmann & Kather, 2010). While the heat of desorption is constant at a fixed temperature, the heat of vaporisation and the sensible heat show a more significant dependency on the CO_2 loading. At a fixed carbon capture rate, the heat of vaporisation slightly reduces with lean loading as the equilibrium partial pressure of CO_2 increases. This results in a reduction in the amount of steam which is to be vaporized (Freguia & T. Rochelle, 2003). However, the sensible heat has an opposite trend due to the increased liquid solvent flow rate required to achieve the CO_2 capture efficiency target. Owing to the trade-off between latent and sensible heats, the reboiler duty is minimized by a certain lean loading value that depends on the operating conditions of the absorption system and the flue gas to be treated (Carapellucci, et al., 2015; Mac Dowell & Shah, 2013). The reboiler temperature remains at about 125 °C, ensuring a negligible MEA degradation (Warudkar, et al., 2013).

Various CO_2 capture efficiencies are achieved by manipulating the lean solvent flow rate in the absorber. This will consequently affect the total rich solvent flow rate into the stripper and thus, the reboiler heating load. The effect of lean solvent flow rate on CO_2 capture efficiency is depicted in Figure 8. An increase in solvent flow rate will result in an improved capture efficiency; however, more dissolved CO_2 will, in return, be needed to be stripped off of the rich solvent, leading to an increase in reboiler duty.

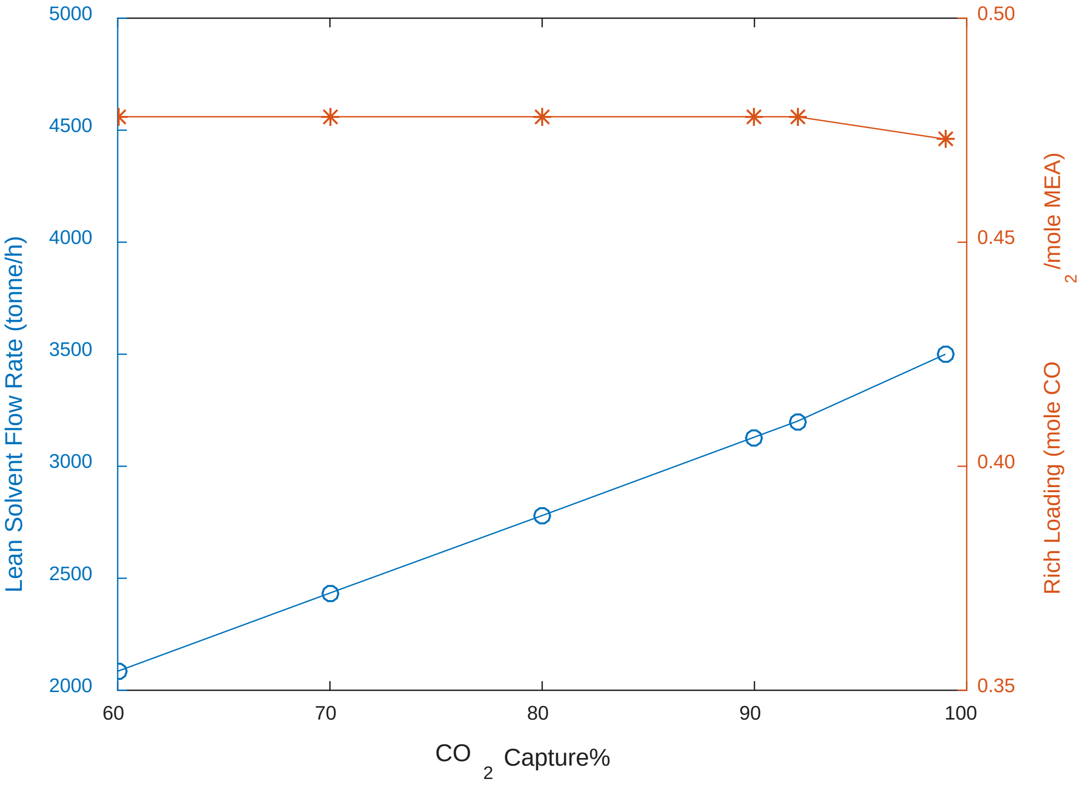

Figure 7: Effect CO_2 capture on required lean solvent flow rate and rich loading (Inlet flue gas with 4 mol% CO_2; 0.21 Lean Loading; 30 wt% MEA)

The heating supply to the reboiler is typically obtained by bleeding steam from between the intermediate and low pressure turbines in the Rankine cycle within the CCGT plant. In our simulation, a saturated steam at 140 - 160 °C is used to model the reboiler heating duty requirements (assuming total condensation and no further sub-cooling) and was therefore, integrated as the utility stream into our simulated process. This is equivalent to a ratio of 1.93 – 1.98 $\frac{kg\ steam}{kg\ CO_2 removed}$ for 90% CO_2 capture, within the range of 1.9 - 2.5 $\frac{kg\ steam}{kg\ CO_2 removed}$ (Idem, et al., 2009) reported in the literature. Obviously the conditions at which the steam is available effects the quantity required; Table 5 presents the impact of varying extraction conditions on the quantity of steam required.

Table 5: Required saturated steam flow rate to heat the reboiler supplied from some IP-LP crossover steam (4 mol% CO2, 30 wt% MEA, 0.21 lean loading, 90% Capture).

Pressure (bar)	**Temperature (°C)**	**Required Steam Flow Rate (kg/s)**	$\frac{\boldsymbol{kg\ steam\ used}}{\boldsymbol{kg\ recovered\ CO_2}}$
3.615	140	97.12	1.93
4.761	150	98.54	1.95
6.182	160	100.05	1.98

3.4 Parasitic Power Loss and Power Plant De-rating

Whilst the ${kg_{steam}}/{kg_{CO_2}}$ is an accessible measure of cost of CCS, expressing this in terms of the reduction in electricity generated is a much more meaningful measure of cost. This is the purpose of this section, and the parameters used to evaluate the power plant de-rating are compiled in Table 6.

Table 6: Parameters used in order to evaluate the parasitic power loss (Zhou & Turnbull, 2002)

Parameter	**Inlet to the LP turbine**	**Outlet of the LP turbine**
Steam pressure (bar_a)	3.615 (saturated)	0.05
Steam temperature (°C)	140	32.8991 (calculated)

Considering an isentropic expansion of steam within the turbine, the quantity of steam required to generate one unit of electricity depends on the inlet and outlet conditions of steam as well as the efficiency of the turbine. This relationship is formulated as (Warudkar, et al., 2013; Ganapathy, 1994):

$$Q_{Gen}(kW) = \Delta H \left(\frac{kJ}{kg}\right).\dot{m}_s\left(\frac{kg}{s}\right).\eta_t \quad (16)$$

Where ΔH is the enthalpy drop across the turbine, $\dot{m}_s$ is the steam flow rate, η_t is the turbine efficiency. The power loss of the power plant is illustrated in Figure 9. There is a 5.2% reduction in net power output for a 90% capture rate, assuming an advanced CCGT with an HHV efficiency of 52% (Won, et al., 2015; Adams & Mac Dowell, 2016). Assuming that this constitutes approximately 60% of total energy penalty (Kothandaraman, et al., 2009), the total reduction in electricity generated by the power plant would be approximately 8-7%-pts, in line with previous estimates (Wang, et al., 2016).

A final measure for evaluating the impact of CCS on a power plant is the energy penalty per MWh of low carbon energy produced. A comparison between the energy efficiency of gas- and coal-fired power plants with CCS is provided here by considering the regeneration energy consumption by the CCS plant per tonne of captured CO_2. This can also be converted into the regeneration energy consumption per unit of electricity produced in the power plant:

$$B\left(\frac{GJ}{MWh}\right) = A\left(\frac{GJ}{t_{CO_2}}\right) \times \frac{F\left(\frac{t_{CO_2}}{MWh}\right)}{\eta} \times \frac{C}{100} \quad (17)$$

Where, A is the regeneration energy consumed by the stripper's reboiler, C is the CO_2 capture rate, F is the amount of CO_2 produced in order to generate one MWh of thermal energy and η is the power plant's efficiency. Table 7 shows the regeneration energy demand for a CCGT and coal-fired power plant.

Table 7: Comparison of regeneration energy consumption: 600 MW coal and CCGT plants with 90% CO_2 capture (no EGR)

CCGT Power Plant		**Coal (bituminous)- fired Power Plant**	
GJ/t_{CO2}	GJ/MWh	GJ/t_{CO2}	GJ/MWh
3.98	1.50	3.90	2.33

Assuming a modern CCGT (60% HHV efficiency) and an advanced ultra-supercritical coal-fired plant (48% HHV efficiency) of the same capacity (*i.e.*, 600 MW), these results show that whilst gas CCS (3.98 GJ/t_{CO2}) incurs a greater energy penalty per tonne of CO_2 captured than coal CCS (3.9 GJ/t_{CO2}), the energy penalty per unit of low carbon power generated is significantly lower for gas-CCS (1.5 GJ/MWh) than for coal (2.33 GJ/MWh).

4 Conclusions

In this study, we have simulated an MEA-based post-combustion CO_2 capture process applied to a 600 MW natural gas-fired power plant with exhaust gas recycle. We found that using a 30 wt% MEA solution and an EGR of 40% to capture 90% of the CO_2 incurred an energy penalty of 3.98 $\frac{GJ\ reboiler\ energy}{tonne\ CO_2\ captured}$. A flow of saturated LP steam at 140 - 160 °C was used to supply the reboiler duty, and therefore required 1.93 – 1.98 $\frac{kg\ steam}{kg\ captured\ CO_2}$. It was observed that there is a well-defined optimum value in the lean loading in the range 0.19 – 0.21, varying primarily as a function of amine concentration and secondly as a function of EGR (*i.e.*, gas-phase CO_2

concentration). Our results also indicate that whilst gas CCS will require more energy, or will be more costly, per tonne of CO_2 captured, than coal CCS, it will require appreciably less energy, or be much less costly, per MWh of low carbon power produced, which is after all, the point.

Acknowledgement

This work was funded by Gas-FACTS EPSRC project grant EP/J020788/1, CO_2QUEST EU FP7 Grant agreement 309102 and MESMERISE-CCS EPSRC EP/M001369/1.

References

Llano-Restrepo, M. & Araujo-Lopez, E., 2015. Modeling and simulation of packed-bed absorbers for post-combustion capture of carbon dioxide by reactive absorption in aqueous monoethanolamine solutions. *International Journal of Greenhouse Gas Control,* Volume 42, p. 258–287.

Abu-Zahra, M., Niederer, J., Feron, P. & Versteeg, G., 2007b. CO_2 capture from power plants: Part II. A parametric study of the economical performance based on mono-ethanolamine. *International Journal of Greenhouse Gas Control,* Volume 1, pp. 135-142.

Abu-Zahra, M. R. et al., 2007a. CO_2 capture from power plants Part I. A parametric study of the technical performance based on monoethanolamine. *International journal of greenhouse gas control,* Volume 1, pp. 37-46.

Adams, T. & Mac Dowell, N., 2016. Off-design point modelling of a 420 MW CCGT power plant integrated with an amine-based post-combustion CO_2 capture and compression process. *Applied Energy,* Volume 178, pp. 681-702.

Akram, M. et al., 2016. Performance evaluation of PACT Pilot-plant for CO_2 capture from gas turbines with Exhaust Gas Recycle. *International Journal of Greenhouse Gas Control,* Volume 47, p. 137–150.

Akram, M., Khandelwal, B., Blakey, S. & Wilson, C. W., 2013. *Preliminary calculations on post combustion carbon capture from gas turbines with flue gas recycle.* San Antonio, ASME Proceedings, p. V01BT04A004.

Alhajaj, A., Mac Dowell, N. & Shah, N., 2016. A techno-economic analysis of post-combustion CO_2capture andcompression applied to a combined cycle gas turbine: Part I. Aparametric study of the key technical performance indicators. *International Journal of Greenhouse Gas Control,* Volume 44, pp. 26-41.

Ali, U. et al., 2016. Techno-economic process design of a commercial-scale amine-based CO_2 capture system for natural gas combined cycle power plant with exhaust gas recirculation. *Applied Thermal Engineering,* Volume 103, pp. 747-758.

Boot-Handford, M. E. et al., 2014. Carbon capture and storage update. *Energy & Environmental Science,* 7(1), pp. 130 - 189.

Canepa, R., Wang, M., Biliyok, C. & Satta, A., 2013. Thermodynamic analysis of combined cycle gas turbine power plant with post-combustion CO_2 capture and exhaust gas recirculation. *Journal of Process Mechanical Engineering,* 227(2), pp. 89-105.

Carapellucci, R., Giordano, L. & Vaccarelli, M., 2015. Studying heat integration options for steam-gas power plants retrofitted with CO_2 post-combustion capture. *Energy,* Volume 85, p. 594–608.

Chen , C. C. & Evans, L. N., 1986. A local composition model for the excess gibbs energy of aqueous electrolyte systems. *AIChE Journal,* Volume 32, pp. 444-454.

Climent Barba, F. et al., 2016. A technical evaluation, performance analysis and risk assessment of multiple novel oxy-turbine power cycles with complete CO_2 capture. *Journal of Cleaner Production,* Volume 133, pp. 971-985.

Dash, S. K., Samanta, A. N. & Bandyopadhyay, S. S., 2011. (Vapour + liquid) equilibria (VLE) of CO_2 in aqueous solutions of 2-amino-2-methyl-1-propanol: New data and modelling using eNRTL-equation. *J. Chem. Thermodynamics,* 43(8), p. 1278–1285.

Department of Energy & Climate Change, 2015. *GOV.UK.* [Online]
Available at: https://www.gov.uk/government/news/new-direction-for-uk-energy-policy
[Accessed 22 8 2016].

Dutta, R., O. Nord, L. & Bolland, O., 2017. Prospects of using equilibrium-based column models in dynamic process simulation of post-combustion CO_2 capture for coal-fired power plant. *Fuel,* Volume 15, p. 85–97.

Freguia, S. & T. Rochelle, G., 2003. Modeling of CO_2 capture by aqueous monoethanolamine. *AIChE Journal,* 49(7), p. 1676–1686.

Ganapathy, V., 1994. *Steam plant calculations manual.* New York: CRC Press.

Gaspar, J. & Fosbøl, P. L., 2015. A general enhancement factor model for absorption and desorption systems: A CO_2 capture case-study. *Chemical Engineering Science,* Volume 138, pp. 203-215.

Hanak, D. P., Biliyok, C. & Manovic, V., 2015. Efficiency improvements for the coal-fired power plant retrofit with CO_2 capture plant using chilled ammonia process. *Applied Energy,* Volume 151, pp. 258-272.

Hassan, B., Ogidiama, O. V., Khan, M. N. & Shamim, T., 2017. Energy and exergy analyses of a power plant with carbon dioxide capture using multistage chemical looping combustion. *Journal of Energy Resources Technology,* 139(3), pp. 032002(1)-32002(9).

Heuberger, C. F., Staffell, I., Shah, N. & Mac Dowell, N., 2016. Quantifying the value of CCS for the future electricity system. *Energy & Environmental Science,* Volume 9, pp. 2497-2510.

Idem, R., Gelowitz, D. & Tontiwachwuthikul, P., 2009. Evaluation of the performance of various amine based solvents in an optimized multipurpose technology development pilot plant. *Energy Procedia,* Volume 1, pp. 1543-1548.

Kehlhofer, R., Hannemann, F., Stirnimann, F. & Rukes, B., 2009. *Combined-cycle gas & steam turbine power plants.* 3rd ed. Tulsa: PennWell.

Kothandaraman, A. et al., 2009. Comparison of solvents for post-combustion capture of CO_2 by chemical absorption. *Energy Procedia,* 1(1), pp. 1373-1380.

Krishnamurthy, R. & Taylor, R., 1985a. A nonequilibrium stage model of multicomponent separation processes. Part I: Model description and method of solution. *AIChE Journal,* 31(3), p. 449–456.

Krishnamurthy, R. & Taylor, R., 1985b. A nonequilibrium stage model of multicomponent separation processes. Part II: Comparison with experiment. *AIChE Journal,* 31(3), p. 456–465.

Kvamsdal, H. M. et al., 2014. Energetic evaluation of a power plant integrated with a piperazine-based CO_2 capture process. *International Journal of Greenhouse Gas Control,* Volume 28, pp. 343-355.

Li, H. et al., 2011. Impacts of exhaust gas recirculation (EGR) on the natural gas combined cycle integrated with chemical absorption CO_2 capture technology. *Energy Procedia,* Volume 4, pp. 1411-1418.

Linnenberg, S. et al., 2012. Evaluating the impact of an ammonia-based post-combustion CO_2 capture process on a steam power plant with different cooling water temperatures. *International Journal of Greenhouse Gas Control,* Volume 10, pp. 1-14.

Lin, Y.-J., Chen, E. & Rochelle, G., 2016. Pilot plant test of the advanced flash stripper for CO_2 capture. *Faraday Discussions,* Volume DOI: 10.1039/c6fd00029k.

Loud, R. & Slaterpryce, A., 1991. *Gas Turbine Inlet Air Treatment,* New York: GE Company - GER-3419A.

Luo, X., Wang, M. & Chen, J., 2015. Heat integration of natural gas combined cycle power plant integrated with post-combustion CO_2 capture and compression. *Fuel,* Volume 151, p. 110–117.

Mac Dowell, N., Samsatli, N. J. & Shah, N., 2013. Dynamic modelling and analysis of an amine-based post-combustion CO_2 capture absorption column. *International Journal of Greenhouse Gas Control,* Volume 12, p. 247–258.

Mac Dowell, N. & Shah, N., 2013. Identification of the cost-optimal degree of CO_2 capture: An optimisation study using dynamic process models. *International Journal of Greenhouse Gas Control,* Volume 13, pp. 44-58.

Mac Dowell, N. & Shah, N., 2014. Dynamic modelling and analysis of a coal-fired power plant integrated with a novel split-flow configuration post-combustion CO_2 capture process. *International Journal of Greenhouse Gas Control,* Volume 27, p. 103–119.

Mac Dowell, N. & Shah, N., 2015. The multi-period optimisation of an amine-based CO_2 capture process integrated with a super-critical coal-fired power station for flexible operation. *Computers & Chemical Engineering,* Volume 74, p. 169–183.

Merkel, T. C. et al., 2013. Selective exhaust gas recycle with membranes for CO_2 capture from natural gas combined cycle power plants. *Industrial and Engineering Chemistry Research,* 52(3), p. 1150–1159.

Mertens, J., Helene , L., Dominique , D. & Thielens, M.-L., 2013. Understanding ethanolamine (MEA) and ammonia emissions from amine based post combustion carbon capture: Lessons learned from field tests. *International Journal of Greenhouse Gas Control,* Volume 13, pp. 72-77.

Mondal, B. K., Bandyopadhyay, S. S. & Samanta, A. N., 2015. Vapor–liquid equilibrium measurement and ENRTL modeling of CO_2 absorption in aqueous hexamethylenediamine. *Fluid Phase Equilibria,* Volume 402, pp. 102-112.

National Energy Technology Laboratory (NETL), 2013. *Cost and performance baseline for fossil energy plants volume 1: bituminous coal and natural gas to electricity,* s.l.: United States Department of Energy.

Norouzbahari, S., Shahhosseini, S. & Ghaemi, A., 2016. Chemical absorption of CO_2 into an aqueous piperazine (PZ) solution: Development and validation of a rigorous dynamic rate-based model. *RSC Advances,* 6(46), pp. 40017-40032.

Oexmann, J. & Kather, A., 2010. Minimising the regeneration heat duty of post-combustion CO_2 capture by wet chemical absorption: The misguided focus on low heat of absorption solvents. *International Journal of Greenhouse Gas Control,* 4(1), p. 36–43.

Ogawa, T., 2013. Carbon dioxide capture and utilization for gas engine. *Energy and Power Engineering,* Volume 5, pp. 587-590.

Oko, E., Wang, M. & Olaleye, A. K., 2015. Simplification of detailed rate-based model of post-combustion CO_2 capture for full chain CCS integration studies. *Fuel,* Volume 142, p. 87–93.

Qi, L. E., 2007. *Aspen HYSYS simulation of CO_2 removal by amine absorption from a gas based power plant.* Gøteborg, SIMS2007 Conference.

Renon, H. & Prausnitz, . J. M., 1968. Local composition on thermodynamic excess functions for liquid mixtures. *AIChE Journal,* 14(1), pp. 135-144.

Rochelle, G. T., 2007. *CO_2 capture by aqueous absorption and stripping..* ABMA Annual Meeting, s.n.

Sharifzadeh, M. & Shah, N., 2015. Comparative studies of CO_2 capture solvents for gas-fired power plants: Integrated modelling and pilot plant assessments. *International Journal of Greenhouse Gas Control,* Volume 43, p. 124–132.

Sherman, B. J., Ciftja, A. F. & Rochelle, G. T., 2016. Thermodynamic and mass transfer modeling of carbon dioxide absorption into aqueous 2-piperidineethanol. *Chemical Engineering Science,* Volume 153, p. 295–307.

Soave, G., 1972. Equilibrium constants from a modified Redkh-Kwong equation of state. *Chemical Engineering Science,* Volume 27, pp. 1197-1203.

U.S. Energy Information Administration, 2015. *US Energy Information Administration.* [Online]
Available at: https://www.eia.gov
[Accessed May 2016].

United Nations, F. C. o. c. C., 2015. *Adoption of the Paris agreement.* [Online]
Available at: https://unfccc.int/resource/docs/2015/cop21/eng/l09r01.pdf
[Accessed 07 04 2016].

US Environmental Protection Agency, 2016. *EPA.* [Online]
Available at: https://www.epa.gov/ghgemissions/global-greenhouse-gas-emissions-data
[Accessed 13 09 2016].

Wang, T. et al., 2016. Enhanced CO_2 absorption and desorption by monoethanolamine (MEA)-based nanoparticle suspensions. *Industrial & Engineering Chemistry Research,* Volume 55, p. 7830−7838.

Warudkar, S. S., Cox, K. R., Wong, M. S. & Hirasaki, G. J., 2013. Influence of stripper operating parameters on the performance of amine absorption systems for post-combustion carbon capture: Part I. High pressure strippers. *International Journal of Greenhouse Gas Control.*

Won, J., Son, C. & Kim, C., 2015. *The performance analysis of a combined power plant implementing technologies for enhancing power and efficiency.* Montreal, Proceedings of ASME Turbo Expo 2015: Turbine Technical Conference and Exposition.

Young, E. K. et al., 2012. Comparison of carbon dioxide absorption in aqueous MEA, DEA, TEA, and AMP solutions. *Bulletin of the Korean Chemical Society,* 34(3), p. 783.

Zhou, S. & Turnbull, A., 2002. *Steam turbine operating conditions, chemistry of condensates, and environment assisted cracking – A critical review,* s.l.: National Physical Laboratory (NPL).